PCCP

Accepted Manuscript

ROYAL SOCIETY OF CHEMISTRY

www.rsc.org/pccp

Journal Name

RSCPublishing

Cite this: DOI: 10.1039/xoxxoooooox

Experimental and theoretical study of the photoisomerization and thermal reversion on 5-arylmethylene-2-thioxoimidazolidin-4-one

A.J. Pepino,[a] M. A. Burgos Paci[a]*, W. J. Peláez[a] and G. A. Argüello[a]

Received ooth January 2012,
Accepted ooth January 2012

DOI: 10.1039/xoxxoooooox

www.rsc.org/

Unraveling the photochemical behaviour of the Green Fluorescent Protein chromophore has lately attracted widespread attention among scientists. In this paper we present the study of the photochemical isomerization Z→E and back reaction of the chromophore analog 5-arylmethylene-2- thioxoimidazolidin-4-one. Experimental results are supported with ab-initio calculations at the DFT, (B3LYP/6-31+g(d,p)), TD-DFT (B3LYP/6-311++g(3df,3pd)) and CASSCF levels. A first excitation to the S_2 state, where the isomerization occurs, is proposed followed by two conical intersections to S_1 and S_0 respectively. Three different mechanisms were analyzed for thermal reversion, concluding that the preferred channel involves an intersystem crossing between the S_0 and T_1 states with formation of a biradical.

Introduction

One of the most relevant photochemical processes in molecular biology is the photoinduced *Z*/*E* (*cis*/*trans*) isomerization occurring in photoreceptors where a protein cofactor converts light energy into work to optimize the reaction channels of biological importance.[1–12] Biological systems use photoisomerization to trigger large amplitude motion in molecular photo-switches[13-14] and to induce peptide folding,[15-17] to control ion complexation or to regulate transport properties of ion channels. Discovery of these processes has encouraged the design of clever synthetic strategies to look for new molecules having the possibility of photoisomerization to imitate the natural behaviour and to understand every detail of the reaction mechanism.

Stilbene and azobenzene represent the most studied cases of photoisomerization investigated both experimentally and theoretically.[18-21]In recent years, some chromophores like the Green Fluorescent Protein Chromophore[22-26]and 11-retinal choromophore in rhodopsin[28] have been the subject of several works. In all cases, photoisomerization is described as a process involving a conical intersection (CI) between two electronic potential energy surfaces. Theoretical and experimental investigation of the role played by these CIs in a photo-chemical reaction is currently a subject of great interest[27].

The mechanism of thermal reverse isomerization has been the subject of controversy. Magee, Shand, and Eyring[29] have proposed two alternatives: isomerization either through formation of a biradical (on a triplet surface) or in the ground state (S_0) by rotation about the C=C bond. Some works agree with the first theory[30-32] whereas other results were more consistent with the second mechanism.[33–35] In 1984 Buechele *et al.*[36] suggested an alternative *cis*/*trans* isomerization pathway for conjugated dienes which involves the formation of a transient intermediate through tautomerization.

The existence of a more complex mechanism has been highlighted in recent works. Vengris *et al.*[37] measured thermal isomerization rates of the representative *E* protein chromophore p-hydroxybenzylidene-dimethyl-imidazolinone (HOBDI) following photoisomerization from the *Z* form and obtained a barrier of 13.1 kcal mol^{-1} for the process. Surprisingly, a high-level ab initio calculation from Weber *et al.*[38] produced an activation energy of 57 kcal mol^{-1}. To gain further insight into this process, Dong *et. al.* [22] studied the thermal isomerization of *cis*-XBDI in a variety of solvents, using substituents that are either electron donors or acceptors. The obtained results are congruent with an addition/elimination mechanism. On the other hand, a theoretical study about *cis*/*trans* isomerization in azobenzene suggests that thermal isomerization proceeds via the non-adiabatic torsion route involving the S_0-T_1-S_0 crossing, the same mechanism already proposed for other systems in 1940[21]. As it can be seen, there is not a single mechanism for isomerization.

To the best of our knowledge there is no study on the *Z*/*E* isomerization mechanism of 5-arylmethylene-2-thioxoimidazolidin-4-ones. The pharmaceutically active properties of the 5-arylmethylene-2-thioxoimidazolidin-4-one

nucleus as antimycobacterial,[39] immunomodulator,[40] anticonvulsant[41] and antifungal[42] have encouraged the development of improved methods for their synthesis and examination of their reactivity. It is known that they can exist in their *Z* and *E* forms, the former being the most stable; however, there are no studies which explain that stability and the conversion mechanism. In a recent paper, [43] we have reported a way of obtaining 5-arylmethylene-3-phenyl-2-thioxoimidazolidin-4-one through selective dehydrogenation of the corresponding 5-benzyl-3-phenyl-2-thioxoimidazolidin-4-one.

In this work we present the photochemical *Z*→*E* isomerization and thermal reversion (**Scheme 1**),of 5-arylmethylene-2-thioxoimidazolidin-4-one (**1**) supporting our experimental results with ab initio calculations at the CASSCF level. The reaction coordinate was simulated in the ground and excited states (S_0, S_1, S_2, and T_1). Three different mechanisms were proposed for thermal reversion, and we concluded that the best-suited one involves the formation of a biradical, which is explained by an intersystem crossing (ISC) between S_0 and T_1 states.

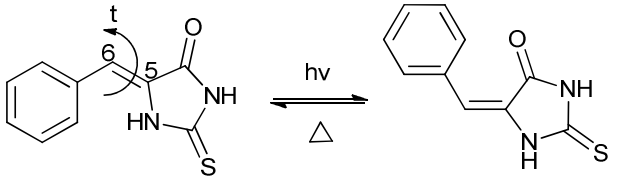

1Z 1E

Scheme 1. Photoisomerization and thermal reversion of 5-arylmethylene-2-thioxoimidazolidin-4-one (1)

Materials and Methods

Synthesis of **1** was performed according to the previously described methodology [44], which yielded the ***1Z/1E*** isomers in a 98:2 proportion in good yields.

The isomer mixture was purified by Preparative Thin-Layer Chromatography (Prep TLC) using chloroform/ethanol (95:5) as solvents to isolate the *Z* and *E* compounds. Both of them were characterized by means of standard spectroscopic techniques (^{1}H NMR, ^{13}C NMR, HMBC, HSQC), UV, IR and mass spectrometry, all data being in agreement with the proposed structures.

Absorption spectra of the solution were recorded on a UV-1601 Shimadzu spectrophotometer using a quartz cell with an optical path length of 1 cm.

Infrared spectra of the solid were recorded on an FTIR Bruker IFS 28 spectrophotometer, with a resolution of 2 cm^{-1} in a range of 4000 to 400 cm^{-1} using KBr disks.

^{1}H, ^{13}C, HSQC and HMBC spectra were recorded in DMSO-d_6 and acetone-d_6 on a Bruker Avance II 400 MHz spectrometer (BBI probe, z gradient) (^{1}H at 400.16 MHz and ^{13}C at 100.56 MHz). Chemical shifts are reported in parts per million (ppm) downfield from TMS. The spectra were measured at 22 ºC.

Gas chromatography/mass spectrometry (GC/MS) analyses were performed on a Shimadzu GC-MS-QP 5050 spectrometer equipped with a VF column (30 m × 0.25 mm × 5 μ), using helium as eluent at a flow rate of 1.1 mL/min. The injector and ion source temperature was 280 ºC, the oven heating ramp was 15 ºC/min from 150 ºC up to 280 ºC, and the interface temperature was 280 ºC. The pressure in the MS instrument was 10^{-5}torr, precluding ion-molecule reactions from taking place, and MS recordings were made in the electron impact mode (EI) at an ionization energy of 70 eV.

Photolyses were carried out using either a black lamp (λ=366nm) or a frequency tripled Nd:YAG laser (Quantel Brillant-B, 355nm; 10Hz) focused on a quartz cell, achieving a maximum energy of 17mJ/pulse. Different solvents were used: acetonitrile (CH_3CN), chloroform ($CHCl_3$) and methanol (CH_3OH), and the reaction was followed by UV spectroscopy.

Fluorescence spectra were measured with a PTI QM2 (Quanta Master 2) spectrofluorometer from Photon Technology International which utilizes a pulsed Xe lamp (75 W) as excitation source and a photon-counting detector. Different solvents were employed: CH_3CN, $(CH_3)_2SO$, dichloromethane (CH_2Cl_2), hexane, and water. An excitation wavelength of 340 nm was used and the emission fluorescence spectra were recorded at 370–600 nm.

Thermal reversion was monitored *in situ* using UV spectroscopy and a thermostatizable cell between 25–60ºC.

We have used ab initio quantum chemistry to investigate the electronic structure of **1** and to describe the potential energy surfaces. No symmetry restrictions were imposed either on the molecular geometries or the electronic wavefunctions. The optimization and vibrational frequencies of the ground state geometries were performed at B3LYP/6-31+g(d,p) level. IRC calculations were carried out to confirm the transition state structures.

In an attempt to obtain both the ground and the excited electronic states on an equal footing, the state-averaged CASSCF method was used. This method is described by the number of states included in the average (N) and the number of electrons (n) and orbitals (m) included in the active space, and it is abbreviated SA-N-CAS(n/m). The 5 orbitals that constitute the active space include: the π-types HOMO-2 and HOMO-1, the n-type HOMO (mostly π*. All potential energy stationary points, including electronic state minima and electronic state degeneracies were optimized with the SA-2-CAS(6/5) method. We used the 6-31G(d) basis set for all CASSCF calculations. The time-dependent density functional theory (TD-DFT/6-311++g(3df,3pd)) method was used for modeling the energies and properties of electronically excited states. Molecular orbital analyses were performed in order to describe the orbitals involved in the process. We have included the solvent contributions using the PCM solvent model in S_0 and T_1. All calculations were done with Gaussian 09[45].

Results

Photochemical studies

The 5-arylmethylene-2-thioxoimidazolidin-4-one (**1**) shows a strong absorbance in the UV region. The absorbance spectrum was measured in three different solvents: CH_3CN, CH_3OH, and $CHCl_3$ (λ_{max}=356 nm, λ_{max}=354 nm, λ_{max}=352nm respectively). The spectra exhibit a bathochromic effect when increasing the polarity of the media, a fact which correlates with a $\pi \longrightarrow \pi^*$ transition as outlined below by theoretical calculations.

Excitation into the absorption band showed no detectable fluorescence for solutions of **1** in the different solvents employed, indicating that the excited states deactivate very rapidly through a non-radiative channel.

All photochemical experiments were carried out in CH_3CN UV irradiation with a Hg lamp (λ=366nm) or a frequency- tripled Nd:YAG laser (355 nm; 9 ns pulses at 10 Hz) produced a change in the ultraviolet spectra of **1*Z*.** Two isosbestic points were observed with no dependence on the solvent polarity. It was concluded that the change was due to the *Z*⟶*E* isomerization. This was proved by isolation, characterization and comparison with the UV spectra of the **1*E*** isomer (**Figure 1**).

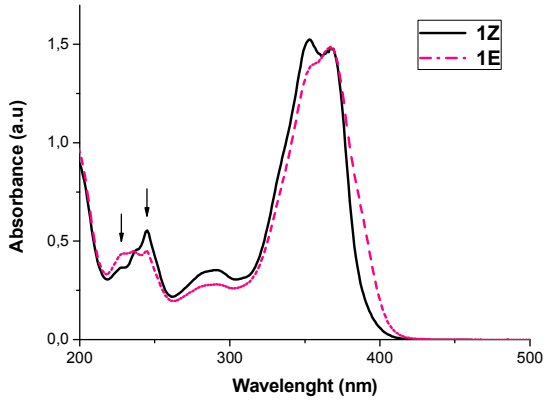

Figure 1. UV-vis absorption spectra of *E* and *Z* isomers of **1** in CH_3CN.

After either 30 seconds with the Hg lamp or about 1000 pulses with the laser, a photostationary state was achieved. **Figure 2** shows the appearance and disappearance of *E and Z* isomers by following the 230 nm and 246 nm bands respectively. By the use of the molar extinction coefficient of each isomer obtained from pure samples the *Z*:*E* ratio of the photostationary state was obtained indicating a 26,5% of *Z*→*E* conversion. A similar value (22%) was achieved by ^{1}H-NMR relative quantification of the benzylic Hydrogen (δ=6.58 and 6.74 ppms for isomers *Z* and *E* respectively).

The isomerization rate was determined from the slope in the linear region of a plot of intensity *vs* laser-irradiation time for the 246 and 230 nm bands. To ascertain whether mono or multiphoton absorption is involved, laser intensity was increased. The plot of the laser power *vs* isomerization rate shows a linear dependence demonstrating that one-photon absorption occurred (**Figure 3**) and that the system is under unsaturated conditions.

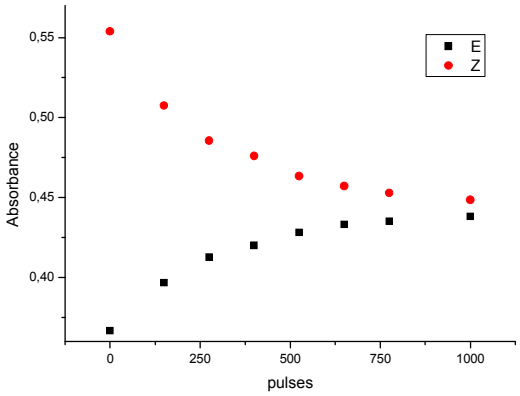

Figure 2. *E* and *Z* isomers formation and consumption.

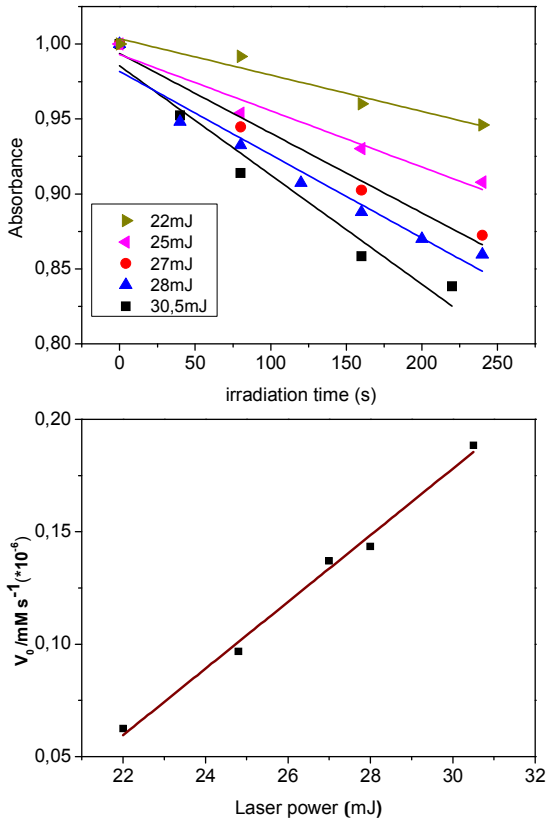

Figure 3. Absorbance of ***1Z*** *vs* irradiation time at different laser power (top). Formation rate of ***1E*** vs laser power (bottom)

Table 1. Rate constants and activation energy for **1*Z*→1*E*** isomerization.

CH_3CN		CH_3OH		$CHCl_3$	
t(ºC)	k (s^{-1})	t(ºC)	k (s^{-1})	t(ºC)	k (s^{-1})
26	$1.4x10^{-5}$	25	$1.6x10^{-5}$	28	$1.7x10^{-5}$
30	$2.3x10^{-5}$	28	$1.9x10^{-5}$	38	$6.4x10^{-5}$
35	$6.0x10^{-5}$	34	$5.7x10^{-5}$	48	$4.5x10^{-4}$
40	$7.6x10^{-5}$	38	$7.5x10^{-5}$	56	$8.3x10^{-4}$
58	$9.3x10^{-4}$	54	$8.4x10^{-4}$	67	$4.3x10^{-3}$
Ea (kcal mol^{-1})	26.7	Ea (kcal mol^{-1})	25.6	Ea (kcal mol^{-1})	27.8
log A	16.0	*log* A	13.9	*log* A	14.6

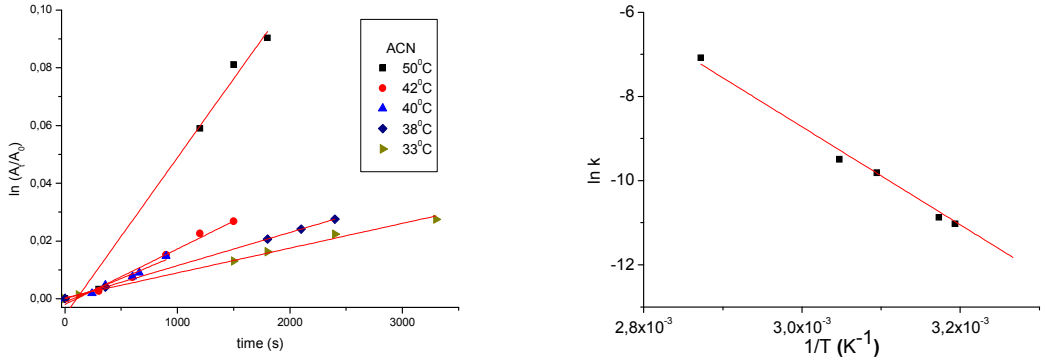

Figure 4.*Left*: Plot of thermal reversion progress in CH_3CN at different temperatures. *Right*: Arrhenius plot

Thermal 1*E*-1*Z* isomerization

Thermal reversion (***1E→1Z***) was monitored *in situ* by UV-Vis spectroscopy using a thermostated cell between 25–67ºC (**Table 1, Figure 4**).

The reaction was studied in a variety of solvents including CH_3OH, $CHCl_3$ and CH_3CN in order to assess the effect of different polarity and nucleophilicity media. **Table 1** shows the rate constant of ***1E→1Z*** isomerization in all cases, and it can be seen that at each temperature the values are the same for the different solvents within experimental error. This finding is opposed to that observed by Dong for Green Fluorescent Protein Chromophores[22] where an addition/elimination mechanism was proposed.

The calculated activation energy and *log* A are about 26 kcal mol^{-1} and 15 respectively. These values are about the same magnitude as those for other *cis*/*trans* isomerizations even though it is known that they strongly depend on the structure of the compounds and their subsitutents.[46] For instance, for 1-deuteriopropene the activation energy and *log* A are 24.7 kcal mol^{-1} and 12.16 respectively[47] and for dideuteriopropene these values are 26.2 and 14.0.[48] However, in conjugated systems, the isomerization process presents lower values of Activation Energy and *log* A (about 13 kcal/mol and 13 respectively).[49] The plot of thermal reversion progress in CH_3CN at different temperatures and the Arrhenius plot are both shown in **Figure 4,** while the corresponding plots for CH_3OH and $CHCl_3$ are in the Supporting Information section.

Mechanisms

We suggest three possible ways of analyzing the thermal mechanism observed: twisting about the τ dihedral through a zwitterionic species (**A**), a 1,3-hydrogen shift (**B**), and a biradical formation (**C**), all of them allowing free rotation through the C_5-C_6 bond (**Scheme 2**).

Ground state B3LYP/6-31+g(d,p) gas-phase calculations show that the 1Z isomer is 2.3 kcal/mol more stable than the 1E. The barrier for the E→Z conversion is 82.3 kcal mol^{-1} through a dihedral τ rotation (**Scheme 2, path A**). The transition state corresponds to a twisted molecule with a 70 º dihedral angle and presents zwitterionic character (μ=13.6 D).

Tautomerization occurs through a 4-membered transition state having an energy barrier of 68.6 kcal mol^{-1} (path **B**), while, the biradical formation involves a barrier of 36.2 kcal mol^{-1} (path **C**). Even the least energetic of the calculated processes has an activation energy higher than the experimental value. Then, in order to get values closer to the experimental ones, we performed other calculations including acetonitrile as solvent and using the PCM model implemented in Gaussian. The energies of the structures which were calculated taking into account the solvent are included in the SI. It can be observed that the activation energies change noticeably for path A (68.1 kcal mol-1), moderately for path B (67.0 kcal mol-1) and there is no change for the biradical channel. The stabilization gained does not bring the activation energies below that of the biradical channel. Besides being the biradical the lowest energy channel, its invariance with the solvent agrees with the experimental results.

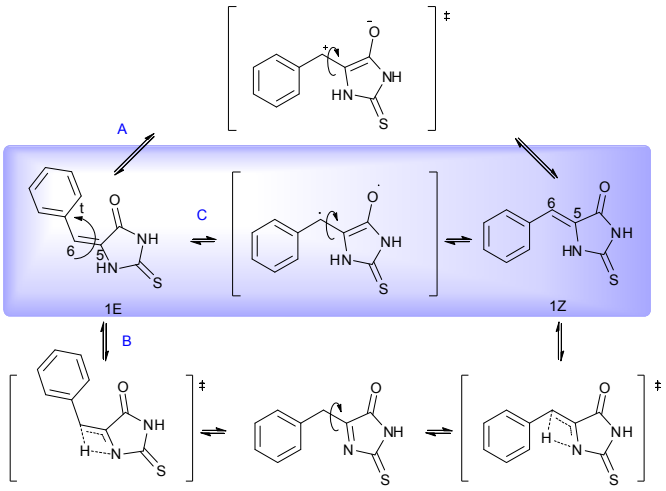

Scheme 2. Suggested mechanisms for thermal **1*Z*/1*E*** isomerization: through a zwitterionic specie (**A**), an 1,3-hydrogen shift (**B**) and a biradical formation (**C**).

The finding that the biradical channel is the preferred one on energetic grounds as well as the closest to the experimental value suggests that thermal isomerization could occur via a triplet state that could be reached through a crossing between S_0 and T_1 surfaces. To assess this postulate and to shed some light on the photochemical behaviour, fully unconstrained optimizations at the CASSCF level were performed.

Types of excitations

First, vertical excitations from the ground-state **1*Z*** minimum (S_0-*Z*) to the S_1 and S_2 excited states were calculated with SA-2-CAS(6/5)/6-31g(d) method, while singlet excitations were recalculated together with their oscillator strength at the TD-DFT (6-311++g(3df,3pd)) level.

Molecular orbital calculations predict that the lowest singlet state (S_1) originates mainly from an n⟶π* excitation while the S_2 has a π⟶π* character. The principal excitations to the S_1 and S_2 states correspond to the HOMO⟶LUMO and to the HOMO-1⟶LUMO transition respectively (**figure 5**).

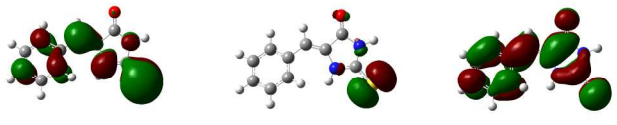

Figure 5. Representation of HOMO-1, HOMO and LUMO of **1**

Oscillator strength values shown in **Table 2** indicate that the absorption maximum at 355 nm is mainly due to excitation to the S_2 state while S_0-S_1 is a forbidden transition. This behaviour is also observed in similar compounds like trans-3-aminostilbene (m-AS), [50] trans-3-(N,N-dimethylamino)stilbene (m-DS)[51], and m-aminobenzylidene-dimethylimidazolinone (m-ABDI).[52] The two aminostilbenes present low intensity S_1 transitions whereas in m-ABDI only a low-lying shoulder is associated with this transition. The effect has been explained in terms of the S_1-S_2 energy gap since its increase comes along with an intensity borrowing from the higher excited state S_2. For m-AS and m-DS the estimated S_1-S_2 energy gaps are 9.0 and 12.3 kcal mol^{-1} ,and the increase parallels the charge transfer character of the S1 state. In our case the calculated S_1-S_2 gap is around 12 kcal mol^{-1} and the S_0-S_1 transition is formally forbidden (see table 2). This could be attributed to the presence of the sulfur atom in the imidazol ring that enhances the charge-transfer character of the S_1 state.

It is important to note that the π⟶π* character of the S_0⟶S_2 transition, which produces the most intense band of the UV spectrum, is congruent with the solvent effect mentioned above where the absorption maximum is shifted to longer wavelengths when the polarity of the media.increases.

Table 2. Absorption Energies (ΔE, kcal mol^{-1}) and Oscillator Strengths (*f*) for the **1*Z*** isomer.

State	1Z		
	SA-2-CAS/ 6-31G(d)	TD-DFT (B3LYP/6-311++G(3df,3pd))	*f*
S_0	0.0	0.0	
S_1	92.9	67.9	0.000
S_2	102.0	80.0	0.700

S_0, S_1, S_2 and T_1 structures and energies

The ground-state (S_0) potential energy surface (PES) along the reaction path that connects reactants and products through the biradical intermediate was recalculated in the gas phase at the CAS(6/5)/6-31g(d) level. The barrier obtained in this case is **77.7 kcal mol^{-1}** relative to the *Z*-conformer in the ground state. All energy values refer to this conformer.

Intrinsic reaction coordinate (IRC) calculations, which were started at the Frank-Condon geometry and computed with the SA-2-CAS(6/5) method on S_2 and S_1 surfaces, gave excited state minima. On the S_2 surface we found two stable structures, one of which corresponds to a twisted geometry with a dihedral τ angle of 50.63º, a relative energy of **93.6 kcal mol^{-1}**, and a C_5=C_6 bond length of 1.456 Å. This structure is 8.4 kcal mol^{-1} below the "planar" (τ 2.256º) Franck-Condon geometry. **Scheme 3** shows that the main reason for the energy relaxation between both geometries is the twisting of the relative positions of the phenyl and imidazole rings. The structure resembles the fluorescence state (FS) minimum reported by Martin *et al.*[53] for the anionic form of HOBDI. The other minimum on the S_2 surface has a *trans* configuration and is the global minimum of this state with a relative energy of **85.2 kcal mol^{-1}**. The main geometrical parameters are a dihedral τ angle of 179.8º and a C_5=C_6 bond length of 1.416 Å. As a general rule, it could be stated that upon excitation of S_2, the C_5-C_6 bond length substantially increases and acquires almost a single bond character. Thus, the rotation about the C_5-C_6 bond could occur in the S_2 state.

The photoisomerization mechanism of GFP chromophores has been explained with a twisted intermediate in the S_1 state that relaxes to both ground state *Z*/*E* structures with similar probabilities. Even in the mechanisms of the meta-Amino systems studied by Cheng et.al.[52] where the excitations are to the S_2 states the main geometrical changes occur in the S_1 state. In the present case, the S_2 state is central to the explanation of the dynamic process of isomerization.

For the S_1 surface there are *Z* and *E* minima (S_1-*Z* and S_1-*E*), the latter being the most stable (**61.6** and **40.0 kcal mol^{-1} respectively**). The geometrical parameters of these structures are, for S_1-*Z*, a dihedral τ angle of 2.2º, a C_5-C_6 bond length of 1.352 Å and a C-C_5-C_6 angle of 129.6º; while for S_1-*E* these values are 171.6º, 1.412 Å and 126.5º respectively. Within this surface, the most important change in geometrical parameters is the C-S bond length (**Scheme 3**, but not shown in the tridimensional plot of **Figure 6**), which increases from 1.653 Å to 1.791 Å as a consequence of the n⟶π* transition.

Otherwise, the optimized PES of T_1 along the torsion pathway has its minimum at roughly 77º where its energy is **55.5 kcal mol^{-1}**. The geometry of this minimum is almost the same as the S_0 maximum, although it is a biradical while the S_0 maximum has a zwitterionic character. **Scheme 3** shows the optimized structure. All the other relevant structures are presented in Supporting Information.

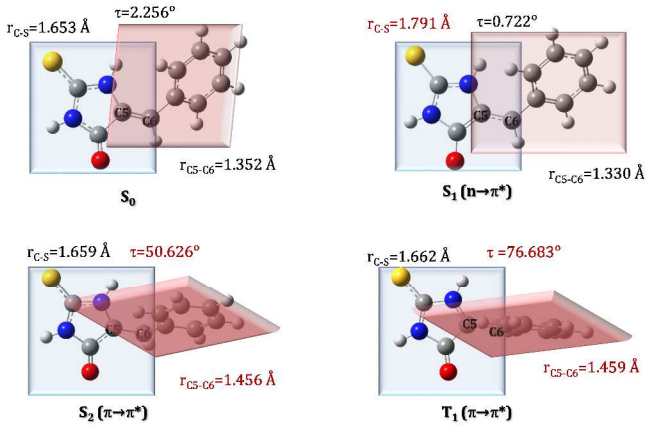

Scheme 3. Geometries of the **1*Z*** isomer on the corresponding minima of S_0, S_1, S_2, and T_1 surfaces

Analysis of the S_1, S_2, and T_1 PES, determination of conical intersections (CI) and intersystem crossings (ISC).

The potential energy curves of S_1, S_2, and T_1 as a function of the torsion dihedral (τ) were obtained. By optimizing the conical intersections we found that the crossing between S_2/S_1 surfaces occurs at the twisted structure with a dihedral τ angle of 117.1º (**91.7 kcal mol^{-1}**) and a C_5-C_6 bond length of 1.455Å. Once on the S_1 surface, the isomerization process continues with a gradual increase in the dihedral until a new conical intersection between S_1 and S_0 at τ 135.0º (**72.8 kcal mol^{-1}**).occurs,The E conformer minimum of the ground state is reached by further relaxation on the S_0 surface (see **Figure 6**).

As stated before, on the way back the system must make its way through an intersystem crossing (only thermal energy near room temperature is responsible for that reversion) at moderate energies. Calculation of the triplet surface gave two points where the crossing could occur, which are shown in **Figure 6**. Within this assumption, thermal **1*E*→1*Z*** isomerization can occur via the T_1 state by overcoming a calculated barrier of approximately 58 kcal mol^{-1} that corresponds to the higher S_0-T_1 crossing (ISC) at the CASSCF level. The experimental activation energy measured in this work is ~26 kcal mol^{-1}. This difference could be attributed to the intrinsic lack of correction for the correlation energy of the method. Precisely, using the B3LYP/6-31+g(d,p) method, where the correlation energy is recovered, the value drops to 36.2 kcal mol^{-1}, which is much closer to the experimental result. Differences of about 10 kcal mol^{-1} between experiment and calculus are a reminder of the approximations employed.

Figure 6 depicts a representation of the S_0, S_1, S_2, and T_1 potential energy surfaces in the space of the two main internal coordinates involved in **1*Z*/1*E*** isomerization (C_5-C_6 bond length and τ torsion). It shows the vertical excitation corresponding to the S_0⟶S_2 transition, the points of minimum energy on each surface, the CI's and the ISC's. Both the direction of photoisomerization and thermal reversion are indicated with arrows.

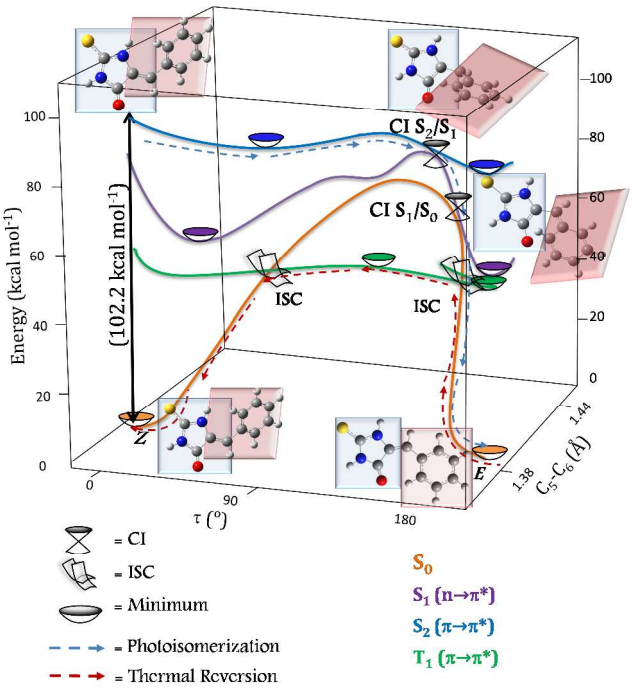

Figure 6. S_0, S_1, S_2 and T_1 potential energy surfaces

The thermal E⟶Z mechanism for the GFP chromophore analogs is being extensively studied and represents a key step in the understanding of the on/off switch of these systems. The direct mechanism has been proposed for example for the 4-methylbenzylidene derivative[54]. However, this rationalization was

rejected because of the strong solvent effect measured for the isomerization reaction through the Hammet formalism. Tolbert's group studied the thermal isomerization of five XBDI derivatives of different donating ability and they obtained a positive correlation with σ which is consistent with a solvent-addition mechanism. Nevertheless, the activation energy measured for the HOBDI was 13.1 kcal mol^{-1} and the authors preferred a tautomerization channel to explain the process. In our case, the activation energy measured is 26 kcal mol^{-1} and the rate constants for the isomerization were not affected, within experimental error, by the different solvents used. All these facts indicate that the isomerization mechanism is strongly dependent on the substituents without a unique path and therefore no general mechanism could be proposed. It must be noted that the activation energies were always lower than those expected for a simple double-bond rotation. In the case of **1,** thermal reversion seems to be assisted by the intersystem crossing between S_0 and T_1 states. This mechanism has been proposed for azobenzene analogs and stilbene The presence of the sulfur atom in the imidazole ring makes the T_1/S_0 gap closer, thus favoring the ISC of both surfaces.

Conclusions

In the present paper the UV photochemical Z⟶E isomerization and the thermal reversion were thoroughly studied experimentally and the results were supported by high-level ab initio calculations. Both isomers were isolated by Preparative Thin-Layer Chromatography and characterized by NMR spectroscopy. The UV-Vis spectrum attributed to each conformer was then used to monitor the photochemical isomerization and the kinetics of the thermal E⟶Z reversion reaction. Illumination of the sample at 355 nm starting with the *Z* isomer produces a photostationary state with 26.5 % of conversion. The kinetics of the thermal reversion process was measured in different solvents, and the kinetic parameters did not show deviations within experimental uncertainties. An activation energy of 26 kcal mol^{-1} was measured for the thermal reversion.

The photochemical process starts with excitation to the S_2 state which corresponds to a π⟶π* transition and the main geometrical changes take place on this surface. A conical intersection to the S_1 surface (n⟶π*) occurs at a twisted geometry and, once there, a barrierless path leads to a S_1/S_0 conical intersection. The thermal reversion involves a biradical formation through a S_0-T_1 intersystem crossing of 58 kcal mol^{-1} in the gas phase which is 20 kcal mol^{-1} less energetic than the simple τ torsion.

The isomerization reaction has been studied for a variety of similar molecules and it seems that there is no general mechanism, probably indicating that intramolecular interactions and different substituents in both rings have crucial effects on the process. In the present case the sulfur atom seems to influence the process by lowering the energy of the T1 state, thus favoring the crossing of the S_0 and T_1 states in an amount that supersedes the solvent effects. In this sense, more studies involving different substituents are desirable to gain insight into this compelling phenomenon.

Acknowledgements
Thanks are due to CONICET, FONCyT, and SECyT-UNC for their financial support. A.J.P. thanks CONICET for her doctoral fellowship. Language assistance by translator Rita Karina Plasencia is gratefully acknowledged.

Notes and references

[a]INFIQC-Dpto. de Fisicoquímica, Facultad de Ciencias Químicas, UNC, Córdoba, Argentina.
*Corresponding author. E-mail: mburgos@fcq.unc.edu.ar

Electronic Supplementary Information (ESI) available: Rate constants obtained by FVP from **7** and **8** (Table S1 and S2), characterization of compounds **7**, **8**, **11**, **12**, **25**, **27**, **28**, **31**, and **35** and Cartesian Coordinates (Å) obtained from the B3LYP(6-31+G(d,p)) computational calculations are provided. See DOI: 10.1039/b000000x/

References

1. J. Dobler, W. Zinth, W. Kaiser and D. Oesterhelt, *Chem. Phys. Lett.*, 1988, **144**, 215-220.
2. R. W. Schoenlein, L. A. Peteanu, R. A. Mathies and C. V. Shank, *Science*, 1991, **254**, 412-415.
3. H. Kandori, Y. Furutani, S. Nishimura, Y. Shichida, H. Chosrowjan, Y. Shibata and N. Mataga, *Chem. Phys. Lett.*, 2001, **334**, 271-276.
4. P. Hamm, M. Zurek, T. Röschinger, H. Patzelt, D. Oesterhelt and W. Zinth, *Chem. Phys. Lett.*, 1996, **263**, 613-621.
5. G. Zgrablic, S. Haacke and M. Chergui, *J. Phys. Chem. B*, 2009, **113**, 4384-4393.
6. M. Chattoraj, B. A. King, G. U. Bublitz and S. G. Boxer, *Proc. Natl. Acad. Sci. U.S.A.,* 1996, **93**, 8362-8367.
7. H. Lossau, A. Kummer, R. Heinecke, F. Po¨ llinger-Dammer, C. Kompa, G. Bieser, T. Jonsson, C. M. Silva, M. M. Yang, D. C. YouvanandM. E.Michel-Beyerle, *Chem. Phys.*, 1996, **213**, 1-16.
8. N. M. Webber, K. L. Litvinenko and S. R. Meech, *J. Phys. Chem. B*, 2001, **105**, 8036–8039.
9. A. Baltuska, I. H. M. van Stokkum, A. Kroon, R. Monshouwer, K. J. Hellingwerf and R. van Grondelle, *Chem. Phys. Lett.*, 1997, **270**, 263-266.
10. H. Chosrowjan, N. Mataga, N. Nakashima, Y. Imamoto and F. Tokunaga, *Chem. Phys. Lett.*, 1997, **270**, 267-274.
11. P. Changenet-Barret, P. Plaza and M. M. Martin, *Chem. Phys. Lett.*, 2001, **336**, 439-445.
12. D. S. Larsen, M. Vengris, I. H. M. van Stokkum, M. A. van der Horst, F. L. de Weerd, K. J. Hellingwerf and R. van Grondelle, *Biophys. J.*, 2004, **86**, 2538-2543.
13. I. K. Lednev, T. Q. Ye, P. Matousek, M. Towrie, P. Foggi, F. V. R. Neuwahl, S. Umapathy, R. E. Hester and J. N. Moore, *Chem. Phys. Lett.*, 1998, **290**, 68-76.
14. T. Nägele, R. Hoche, W. Zinth and J. Wachtveitl, *Chem. Phys. Lett.*, 1997, **272**, 489-495.
15. L. Ulysse, J. Cubillos and J. Chmielewski, *JACS*, 1995, **117**, 8466–8467.
16. S. Rudolph-Bohner, M. Krüger, D. Oesterhelt, L. Moroder, T. Nägele and J. Wachtveitl, *J. Photochem. Photobiol.*, A, **1997**, 105, 235-241.
17. J. Bredenbeck, J. Helbing, A. Sieg, T. Schrader, W. Zinth, C. Renner, R. Behrendt, L. Moroder, J. Wachtveitl and P. Hamm, *Proc. Natl. Acad. Sci.,* USA, 2003, **100**, 6452-6457.
18. G.N. Lewis, T. Magel, D. Lipkin, *JACS*, 1940, **62**, 2973-2980.
19. J. Saltiel, S. Ganapathy, and C. Werking, *J. Phys. Chem.*, 1987, **91**, 2155-2158.
20. J.M. Rodier and A. B. Myers, *JACS*, 1993, **115**, 10791-10795.
21. A. Cembran, F. Bernardi, M. Garavelli, L. Gagliardi, G. Orlandi.*JACS*, 2004, **126**, 3234-3243
22. J. Dong, F. Abulwerdi, A. Baldridge, J. Kowalik, K. M. Solntsev, and L. M. Tolbert, *JACS*, 2008, **130**, 14096-14098.
23. V. Polyakov, B. L. Grigorenko, E. M. Epifanovsky, A. I. Krylov, and A. V. Nemukhin, *J. Chem.TheoryComput.* 2010, **6**, 2377-2387.
24. L. V. Schafer, G. Groenhof, M. Boggio-Pasqua, M. A. Robb, H. Grubmuller, *Computational Biology,* 2008, **4 (3)**, 1-14.

25. (a) K. Addison, J. Conyard, T. Dixon, P. C. B. Page, K. M. Solntsev, S. R. Meech, *J. Phys. Chem. Lett.*, 2012, **3 (16)**, 2298-2302. (b) M. Ikejiri, M. Tsuchino, Y. Chihara, T. Yamaguchi, T. Imanishi, S. Obika, K. Miyashita, *Organic Letters,* 2012, **14 (17)**, 4406-4409.
26. Y. Lei, L. Yu, B. Zhou, C. Zhu, Z. Wen, S. H. Lin, *J. Phys. Chem. A,* 2014 *(ASAP)*
27 D. Polli, O. Weingart, D. Brida, E. Poli, M. Maiuri, K. M. Spillane, A. Bottoni, P. Kukura, R. A. Mathies, G. Cerullo, M. Garavelli. *Angew. Chem. Int. Ed.* 2014, 53, 2504-2507.
28. D. Polli, P. Altoe, O. Weingart, K. M. Spillane, C. Manzoni, D. Brida, G. Tomasello, G. Orlandi, P. Kukura, R. A. Mathies, M. Garavelli, G. Cerullo. *Nature*, 2010,**467**, 440–443.
29. J. L. Magee, W. Shand and H. Eyring. *JACS*, 1941, **63**, 677-688.
30. G. B. Kristiakowsky, M. Z. Nelles, Physik. *Chem. Leipzig, Bodenstein-Festband*, 1931, **8**, 367-369.
31. G. B. Kristiakowsky, W. R. Smith, *JACS*. 1934, **56**, 638-642.
32. G. B. Kristiakowsky, W. R. Smith. *JACS*. 1936, **58**, 766-768.
33. R. B. Cundall. Progr. *Reaction Kinetics*, 1964, **2**, 165-215.
34. B. S. Rabinovitch, K. W. Michel *JACS*, 1959, **81**, 5065-5071.
35. M. C. Lin, K. J. Laidler, *Can. Jour. of Chem.*, 1968, **46**, 973-978.
36. J. L. Buechele, E. Weitz, F. D. Lewis, *J. Phys. Chem.,* 1984, **88**, 868-876.
37. (a) M. Vengris, I. H. M. van Stokkum, X. He, A. F. Bell, P. J. Tonge, R. van Grondelle, D. S. J. Larsen, D. S. Springer Ser. *Chem. Phys.* 2005, **79**, 610-612. (b) M. Vengris, I. H. M. van Stokkum, X. He, A. F. Bell, P. J. Tonge, R. van Grondelle, D. S. J. Larsen, *J.Phys. Chem. A*, 2004, **108**, 4587-4598.
38. Weber, W.; Helms, V.; McCammon, J. A.; Langhoff, P. W. *Proc. Natl. Acad. Sci. U.S.A.* 1999, **96**, 6177-6182.
39. Kieć-Kononowicz K., Szymańska E., *Il Farmaco* 2002, **57**, 909-916.
40. Chazeau V., Cussac M., Boucherle A., *Eur. J. Med. Chem.* 1992, **27**, 625-625.
41. Thenmozhiyal J., Wong P., Chui W., *J. Med. Chem.* 2004, **47**, 1527-1535.
42. Marton J., Enisz J., Hosztafi S., Tímar T., *J. Agric. Food Chem.* 1993, **41**, 148-152.
43. A. J. Pepino, W. J. Peláez, E. L. Moyano, G. A. Argüello, *Eur. J. Org. Chem*., 2012, **18**, 3424-3430.
44. A. J. Pepino, W. J. Peláez, M. S. Faillace, N. M. Ceballos, E. L. Moyano, G. A. Argüello, *RSC advances, sent.*
45. Gaussian 09, Revision B.01, Frisch, M. J.; Trucks, G. W.; Schlegel, H. B.; Scuseria, G. E.; Robb, M. A.; Cheeseman, J. R.; Scalmani, G.; Barone, V.; Mennucci, B.; Petersson, G. A.; Nakatsuji, H.; Caricato, M.; Li, X.; Hratchian, H. P.; Izmaylov, A. F.; Bloino, J.; Zheng, G.; Sonnenberg, J. L.; Hada, M.; Ehara, M.; Toyota, K.; Fukuda, R.; Hasegawa, J.; Ishida, M.; Nakajima, T.; Honda, Y.; Kitao, O.; Nakai, H.; Vreven, T.; Montgomery, Jr., J. A.; Peralta, J. E.; Ogliaro, F.; Bearpark, M.; Heyd, J. J.; Brothers, E.; Kudin, K. N.; Staroverov, V. N.; Keith, T.; Kobayashi, R.; Normand, J.; Raghavachari, K.; Rendell, A.; Burant, J. C.; Iyengar, S. S.; Tomasi, J.; Cossi, M.; Rega, N.; Millam, J. M.; Klene, M.; Knox, J. E.; Cross, J. B.; Bakken, V.; Adamo, C.; Jaramillo, J.; Gomperts, R.; Stratmann, R. E.; Yazyev, O.; Austin, A. J.; Cammi, R.; Pomelli, C.; Ochterski, J. W.; Martin, R. L.; Morokuma, K.; Zakrzewski, V. G.; Voth, G. A.; Salvador, P.; Dannenberg, J. J.; Dapprich, S.; Daniels, A. D.; Farkas, O.; Foresman, J. B.; Ortiz, J. V.; Ioslowski, J.; Fox, D. J. Gaussian, Inc., Wallingford CT, 2010.
46. By Joseph J. Gajewski, 2nd edition, Elsevier, *Hydrocarbon Thermal Isomerizations, 2004***,**pp15.
47. D. K. Lexis, B. Brandt, L. Crockford, D. A. Glenar, G. Rauscher, J. Rodriguez, J. E. Baldwin, *JACS,* 1993, **115**, 11728-11734.
48. M. C. Flowers, N. Jonathan, *J. Chem. Phys.,* 1969, **51**, 2805-2812.
49. W. von E. Doering, W. R. Roth, R. Bauer, H. Boenhe, R. Breuckmann, J. Ruchkamp, O. Wortmann, *Chem. Ber.,* 1991, **124**, 1461-1465.
50. F. D. Lewis, R. S. Kalgutkar, J.-S. Yang, *JACS*, 1999, **121**, 12045-12053.
51. F. D. Lewis, W. Weigel, *J. Phys. Chem. A*, 2000,**104**, 8146-8153.
52. C. W. Cheng, G.-J. Huang, H.-Y. Hsu, C. Prabhakar, Y-P. Lee, E. W.-G Diau, J.-S. Yang, *J. Phys. Chem. B*, 2013, **117**, 2705-2716.
53. M. E. Martin, f. Negri, M. Olivucci, *JACS,* 2004, **126**, 5452-5464.
54. B. Hager, B. Schwarzinger, H. Falk, *Monatsh. Chem.* 2006, **137**,163-168.

